INTEGRATION OF SCHEDULING AND CONTROL UNDER UNCERTAINTIES

By

XIAN WU

A thesis submitted to

Graduate School – New Brunswick

Rutgers, the State University of New Jersey

In partial fulfillment of the requirement

For the degree of

Master of Science

Graduate Program in

Chemical and Biochemical Engineering

Written under the direction of

Marianthi G. Ierapetritou

And approved by

____

____

____

New Brunswick, New Jersey

October, 2015

ABSTRACT OF THE THESIS

Integration of Scheduling and Control under Uncertainties

By XIAN WU

Thesis Director:

Marianthi G. Ierapetritou

The objective of the thesis consists of: (1) analyzing potential uncertainties of the simultaneous integration model of scheduling and control of an isothermal multiproduct continuous flow stirred tank reactor (CSTR), (2) implementing scenario based method to minimize the influence brought by the incorporation of the uncertainties, (3) investigating other promising methods of uncertainty treatments and value the corresponding feasibility. In order to fulfill those goals, this work includes: (1) conducting sensitivity analysis on potential parameters of the integration model, and summarizing the effects brought by the incorporation of uncertainties, (2) applying scenario based method to the integration model to minimize the affect caused by the

introduction of the uncertainties, and evaluating the results, (3) comparing the advantages and disadvantages of other promising uncertainty treatments and predicting the possible developing direction.

ACKNOWLEDGEMENT

Two years' Master Program in Rutgers University is coming to an end, please allow me to express my thankfulness to the people who made my life in Rutgers colorful and meaningful. In the first place, I want to express my sincere gratitude to my thesis advisor, Dr. Marianthi G. Ierapetritou, for her wise and farsighted guidance on starting my research on simulation. Also, I want to thanks to the members of my thesis committee members Dr. Yannis Androulakis and Dr. Meenakshi Dutt, for your attendance. I also want to express my thankfulness to the Ph.D. candidate Jinjun Zhuge, who offered me a lot of help and suggestions during my research. Also, I want to thanks to all the members in the research group, my classmates and the faculties in the department. Finally, I want to thank my families for their consist support.

TABLE OF CONTENTS

LIST OF TABLES

LIST OF ILLUSTRATIONS

Chapter 1 Introduction

With the rapid development of the process system engineering, chemical process simulation has gathered the attention of both scientists and engineers. Simulation has become an indispensable process before conducting experiments in reality. Scheduling optimization, process control optimization, and uncertainty treatments are among the most popular topics associated with process system engineering.

Acting as a decision making method, scheduling has become a crucial process in most of the industrial production, such as chemical industry, petroleum industry, pharmaceutical industry. The main task of the scheduling problem is to obtain the optimal production arrangement with limited resources. For example, in a chemical industry process, the optimal production arrangement must be calculated accurately to make sure that the raw materials, reaction equipment, ancillary utilities and other related resources are not exhausted while achieving the optimal economic goal.[1] Many scientists and engineers have been working on this topic to develop and solving scheduling model more accurately and easily.[2, 3]

As another crucial tool, process control plays a crucial role in many manufacturing industries, including chemical engineering. Process control has two major goals: taking advantages of real time manipulation of specific variables to avoid system disturbances, and ensuring the production meets the corresponding requirements and constraints.

Additionally, process control can also introduce economic or economic-related criteria into determination of the current target values for selected variables.[4]

Under the influence of the globalization, manufacturing industry has to face more challenges to survive the harsh competition. Besides the traditional pressure such as lowering the production cost and increasing productivity, manufacturing industry also has to face an unprecedented challenge – a rapidly changing market.[5] In order to reduce operational cost and make production more flexible to keep up with the profitability, the demand of integration of the production scheduling and system control has become more and more badly.[6]

Sharing the same economic goal, maximizing profit rate or minimizing cost, it is reasonable to predict that the integration of scheduling and control can bring a more promising economic benefit. Furthermore, the formulations of scheduling and control models interacts, which could make the integration process become seamless. Even though the formulations are not same to each other, through mathematical processes, such as discretization, we could bridge those two optimization problems and realize the integration. Unfortunately, production scheduling problem and process control problem have been treated distinctively for quite some time. Trials on integration of these two optimization problems are quite recent.[7]

Another major concern of simulation is the disturbances brought by uncertainties. It is hardly to have no numerical error during the actual process, such as preparing constant concentration reactants or obtaining exact value of variables. Besides, in many works, researchers prefer to assume relatively stable parameters as constants. The original intention is to keep the briefness of the model without losing the accuracy. However, scientists have proven that this assumption is not tenable. The outcome of the model may change dramatically when incorporating those tiny uncertainties into the optimization problem.[8]

In this work, we focused on the robustness of the integration model of scheduling and control of an isothermal multiproduct CSTR when incorporating the uncertain parameters used to be treated as constants. By introducing uncertain kinetic parameter K and the initial concentration of the reactant C_0 into the dynamic part of the integration model, we analyzed the influence of the optimal solution and applied a scenario based method of uncertainty treatment to minimize the influence. Also, we presented and evaluated several promising methods of uncertainty treatment to be applied to the system in the future.

Chapter 2 Integration Model of Scheduling and Control

2.1 Integration of Scheduling and Control

Scheduling models and control models used to be solved individually. However, the simple combination of respective optimal solutions of scheduling model and process control model is not capable of obtaining the optimal solution of the whole process model. To obtain the genuine optimal solution, we should integrate scheduling and process control into one model, and solve for the overall optimal solution. In order to integrate the scheduling model and control model, we chose the profit rate as the objective functions of both models. By combining the objective functions, we obtained the integration model of scheduling and control.

We assume that there is no revenue obtained during the transition between steady states. Therefore, in order to maximize the profit rate, we should reduce the length of transition periods. Generally, process control problems are formulated into a dynamic optimization problem, such as a Mix-Integer Dynamic Optimization (MIDO) problem in this work. Besides, it should be mentioned that the steady state operation data of the integration model is obtained by solving the open loop integration.[9]

In this work, we conducted research on a simultaneous integration model of scheduling and control on an isothermal multiproduct CSTR.[10] The scheduling part of the model was formulated into a Mix-Integer Non-Linear Liner Programming (MINLP) problem. In order to integrate to the scheduling part, the process control part was discretized into an MINLP problem from a Mix-Integer Dynamic Optimization (MIDO) problem by applying the Runge–Kutta Forth-Order Method.

2.2 Integration Model of a Isothermal Multiproduct CSTR

2.2.1 Objective Function

Shown in 2.1, the objective function to be maximized Φ stands for the total profit rate, which is calculated by subtracting the total cost rate of inventory Φ_2 and total cost rate of raw material Φ_3 from the total revenue rate Φ_1.

Expressed in 2.2, the total revenue rate Φ_1 is obtained by summing the revenue rate of each product, which is calculated by multiplying the price of the product C_i^p by the corresponding depletion rate of the products W_i/T_c.

The total inventory cost rate Φ_2, shown as 2.3, is gained from summing the inventory cost of products. The inventory cost of product i is calculated by timing inventory cost rate of product i by the respective inventory accumulation rate. From the beginning to the end of the steady state period, the product accumulation rate can be expressed by the production rate G_i subtracting the depletion rate W_i/T_c. The accumulation rate reaches the highest value while the production time reaches the end of the production period Θ_i. After Θ_i until the end of production cycle, the accumulation rate decreases because the pure deletion of the product with a rate of W_i/T_c. The total rate of the inventory cost can be obtained by the inventory cost rate C_i^s timing the time related stocking amount $\frac{1}{2}T_c\left(G_i - \frac{W_i}{T_c}\right)\Theta_i$.

According to the different periods of production, the rate of total raw materials cost rate Φ_3 is obtained from summing all the raw material cost rate. Raw material cost rate can be segregated into two parts. The first part is the transition period. Within transition period, the rate of raw material cost is calculated by multiplying the unit cost of raw material C^r by the summation of raw material cost of all the transition elements $\sum_{k=1}^{N_s}\sum_{e=1}^{N_e} h_k\theta_k^t(u_{ke}^1 + u_{ke}^2 + u_{ke}^3 + \cdots + u_{ke}^m)$. The second part includes all the raw material cost of steady state periods. During steady states, the rate of raw material cost is obtained by timing C^r by the summation of the raw materials cost of all the steady state elements within the production cycle $\sum_{k=1}^{N_s} p_k\left(\overline{u}_k^1 + \overline{u}_k^2 + \overline{u}_k^3 + \cdots + \overline{u}_k^m\right)$. The expression of the rate of total raw material cost is shown in 2.4.

$$\Phi = \Phi_1 - (\Phi_2 + \Phi_3) \qquad 2.1$$

$$\Phi_1 = \sum_{i=1}^{N_p} \frac{C_i^p W_i}{T_c} \qquad 2.2$$

$$\Phi_2 = \sum_{i=1}^{N_p} \frac{1}{2} C_i^s \Theta_i \left(G_i - \frac{W_i}{T_c}\right) \qquad 2.3$$

$$\Phi_3 = \frac{1}{T_c}\Big[\sum_{k=1}^{N_s}\sum_{e=1}^{N_e} C^r h_k \theta_k^t (u_{ke}^1 + u_{ke}^2 + u_{ke}^3 + \cdots + u_{ke}^m) \qquad 2.4$$

$$+ \sum_{k=1}^{N_s} C^r p_k\left(\overline{u}_k^1 + \overline{u}_k^2 + \overline{u}_k^3 + \cdots + \overline{u}_k^m\right)\Big]$$

2.2.2 Assignment Constraints

Assignment constraints, inheriting from scheduling, play a major role in the determination of optimal production schedule. In this work, we one production cycle has five slots. As expressed in 2.5 and 2.6, we assume that each slot can only be assigned to produce one product, and each product can only be produced once during one production cycle. y_{ik}, a binary variable indicating the product allocation, obtains 1 if and only if product i is produced in slot k, otherwise it equals to 0. Shown in 2.8, y'_{ik} is an auxiliary variable corresponding to y_{ik}. As shown in 2.9 and 2.10, z_{ipk} is a binary variable indicating the assignment of the transition periods, which obtains 1 while the transition from producing product i to producing product p takes place in slot k, otherwise it obtains 0.

$$\sum_{k=1}^{N_s} y_{ik} = 1, \ \ \forall i \qquad 2.5$$

$$\sum_{i=1}^{N_p} y_{ik} = 1, \ \ \forall k \qquad 2.6$$

$$y'_{ik} = y_{i,k-1}, \ \ \forall i, k \neq 1 \qquad 2.7$$

$$y'_{i1} = y_{i,N_s}, \ \ \forall i \qquad 2.8$$

$$z_{ipk} \geq y'_{ik} + y_{pk} - 1, \ \ \forall i, p, k \qquad 2.9$$

$$z_{ipk} \leq y'_{ik}, \ \ \forall i, p, k \qquad 2.10$$

2.2.3 Demand Constraints

Originating from the scheduling, demand constraints regulate the minimum amount of products that meets the market demand. As showed in 2.11, the production rate G_i is obtained by multiplying the flow rate of the CSTR F^0, by the conversion of the corresponding product $(1 - X_i)$. Shown as 2.12, with G_i and Θ_i, we can calculate the actual minimum amount of each product W_i. As to 2.13, shows that the production amount of each product should at least meets its market demand, which are obtained by timing the demand rate D_i by cycle time T_c.

$$G_i = F^0(1 - X_i), \ \forall i \tag{2.11}$$

$$W_i = G_i\Theta_i, \ \forall i \tag{2.12}$$

$$W_i \geq D_iT_c, \ \forall i \tag{2.13}$$

2.2.4 Time Constraints

As typical scheduling problem constraints, time constraints define the process limit of each product and the continuity of the system from the view of time. As shown in 2.14, θ_{ik}, the processing time of product i in slot k should not exceed the maximum time limit θ^{max}. With θ_{ik}, we can get the processing time of product i, Θ_i, as shown in 2.15 and process time at slot k, p_k, as shown in 2.16. θ_k^t, the transition time from product i to product p in slot k, is calculated by timing the estimation time value of transition t_{pi}^t by the binary variable z_{ipk}, which is shown in 2.17. In 2.18, the ending time of the slot k, t_k^e, is obtained by adding the processing time p_k and transition time θ_k^t to the starting time of the slot k, t_k^s. In equation 2.19, we set the initial value of production time t_1^s to be 0. As shown in 2.20, in order to keep the continuity of the integration model, the starting time of slot k t_k^s should equal to the ending time of the previous slot t_{k-1}^e. Additionally, the ending time of each slot should not beyond the cycle time T_c, which is shown in 2.21.

$$\theta_{ik} \leq \theta^{max} y_{ik}, \quad \forall i, k \tag{2.14}$$

$$\Theta_i = \sum_{k=1}^{N_s} \theta_{ik}, \quad \forall i \tag{2.15}$$

$$p_k = \sum_{i=1}^{N_p} \theta_{ik}, \quad \forall k \tag{2.16}$$

$$\theta_k^t = \sum_{i=1}^{N_p} \sum_{p=1}^{N_p} t_{pi}^t \, z_{ipk}, \quad \forall k \tag{2.17}$$

$$t_k^e = t_k^s + p_k + \theta_k^t \tag{2.18}$$

$$t_1^s = 0 \tag{2.19}$$

$$t_k^s = t_{k-1}^e, \quad \forall k \neq 1 \tag{2.20}$$

$$t_k^e \leq T_c, \quad \forall k \tag{2.21}$$

2.2.5 Dynamic Model and Discretization

In this work, we focus on an isothermal multiproduct CSTR, which produces five products, A to E, within one production cycle. The dynamic equation of the reaction is shown in the expression 2.23. Based on the dynamic equation, we take the concentration of the reactant in the system as the state variable x, and the feeding rate of the CSTR as the manipulated variable u.

The products are classified by the concentration of the reactant product. The main reaction in the CSTR is a simple irreversible reaction, which was expressed in 2.22. In the industry, the time scale of the CSTR varies from minute to days. The time scale is determined by several parameters of the system, such as the flow rate of the CSTR, the volume of the CSTR and the reaction rate of the reaction. For most bio-reactors, the reaction rate affects the time scale more, because the reaction rate of bio-process is much slower compared to the chemical process. Therefore, the time scale of fermentation CSTR is always counted by hour or day. Another important application of CSTR is the polymerization process, whose reaction rate is much higher than the bio-reaction, which indicates the flow rate and volume of the reactor are more important. The corresponding time scale is mostly counted by minute to hour. In our case, we assume the reaction in the CSTR is a simple irreversible chemical reaction, and obtain the corresponding time scale as hour. Accordingly, the volume of the CSTR V is set to be 5000 litter. Then we obtain the equation of state as shown in equation 2.24. It should be mentioned that the values of the steady state operation parameters are obtained by solving the open loop model. Those values are listed in Table 2.1.

Table 2.1 Value of Input Data of the Integration Model

Product	**Q (L/hour)**	**CR (mol/L)**	**Demand Rate (kg/hour)**	**Product Price ($/kg)**	**Inventory Cost ($/kg)**
A	10	0.0967	3	200	1
B	100	0.2	8	150	1.5
C	400	0.3032	10	130	1.8
D	1000	0.393	10	125	2
E	2500	0.5	10	120	1.7

To integrate with the scheduling part, we implement the Runge–Kutta Forth-Order Method to discretize the dynamic model from an MIDO problem into an MINLP problem. We set the parameter e as the index of the transition period elements. Shown in 3.30, the scale step length between the elements h_k is obtained from the number of the elements during the each transition period N_e. The actual transition time of slot k θ_k^t is obtainted from the scheduling part of the model. Therefore, the actual step length of the transition period of slot k can be expressed as $h_k\theta_k^t$. In this study, we obtain 60 elements during each transition period. The discretization of the model is expressed in equations from 2.25 to 2.30.

The kinetic parameter K and initial concentration of the reactant C_0 are retreated as a constant parameter originally. In this work, in order to make the integration model closer to the realistic process, we introduce uncertain K and C_0 to the integration model and implement uncertainty treatment to minimize the influence brought by the incorporation of uncertainties.

$$3R \xrightarrow{k} P \qquad 2.22$$

$$\frac{dC_R}{dt} = \frac{Q}{V}(C_0 - C_R) - KC_R^3 \qquad 2.23$$

$$\dot{x}_{ke}^{n} = \frac{u_{ke}^{m}}{V}(C_0 - x_{ke}^{n}) - K{x_{ke}^{n}}^{3}, \forall n, k, e \qquad 2.24$$

$$K_{1}{}_{ke}^{n} = \dot{x}_{ke}^{n} \qquad 2.25$$

$$K_{2}{}_{ke}^{n} = \frac{u_{ke}^{m}}{V}\left(C_0 - \left(x_{ke}^{n} + 0.5h_k\theta_k^t K_{1}{}_{ke}^{n}\right)\right) - K\left(x_{ke}^{n} + 0.5h_k\theta_k^t K_{1}{}_{ke}^{n}\right)^3, \forall n, k, e \qquad 2.26$$

$$K_{3}{}_{ke}^{n} = \frac{u_{ke}^{m}}{V}\left(C_0 - \left(x_{ke}^{n} + 0.5h_k\theta_k^t K_{2}{}_{ke}^{n}\right)\right) - K\left(x_{ke}^{n} + 0.5h_k\theta_k^t K_{2}{}_{ke}^{n}\right)^3, \forall n, k, e \qquad 2.27$$

$$K_{4}{}_{ke}^{n} = \frac{u_{ke}^{m}}{V}\left(C_0 - \left(x_{ke}^{n} + 0.5h_k\theta_k^t K_{3}{}_{ke}^{n}\right)\right) - K\left(x_{ke}^{n} + 0.5h_k\theta_k^t K_{3}{}_{ke}^{n}\right)^3, \forall n, k, e \qquad 2.28$$

$$x_{k,e+1}^{n} = x_{ke}^{n} + \frac{1}{6}h_k\left(K_{1}{}_{ke}^{n} + 2K_{2}{}_{ke}^{n} + 2K_{3}{}_{ke}^{n} + K_{4}{}_{ke}^{n}\right) \qquad 2.29$$

$$h_k = \frac{1}{N_e} \qquad 2.30$$

2.2.6 Initial Condition and System Continuity

Shown in 2.31 and 2.34, the values of state variable and manipulated variable at the very beginning of the production cycle equal to the values of corresponding variables by the end of last production cycle. As to the system continuity, the integration model should also hold the consistency in state variable $x_{k,e}^{n}$ besides the time constraint we mentioned before. To keep continuity, we must make sure the value of $x_{k,e}^{n}$ at the beginning of each slot matches its value by the end of the former slot, which are shown in 2.32 and 2.35. Expressed in 2.33 and 2.36, the desired state variable $\bar{x}_k^n$ and desired manipulated variable $\bar{u}_k^m$ obtain the values of corresponding steady state values.

Besides, as shown in 2.37 to 2.39, to maintain continuity of the system, the values of state variables by the end of the transition match those values at the beginning of the steady state periods. We also set $x_{k,e=1}^n$, the state value of the first transition element of the first slot, the value of the initial state variable $x_{in,k+1}^n$.

$$x_{in,1}^n = \sum_{i=1}^{N_p} x_{ss,i}^n y_{i,N_s}, \ \ \forall n \tag{2.31}$$

$$x_{in,k}^n = \sum_{i=1}^{N_p} x_{ss,i}^n y_{i,k-1}, \ \ \forall n\,, k \neq 1 \tag{2.32}$$

$$\bar{x}_k^n = \sum_{i=1}^{N_p} x_{ss,i}^n y_{i,\mathrm{k}}, \ \ \forall n, k \tag{2.33}$$

$$u_{in,1}^m = \sum_{i=1}^{N_p} u_{ss,i}^m y_{i,N_s}, \ \ \forall m \tag{2.34}$$

$$u_{in,k}^m = \sum_{i=1}^{N_p} u_{ss}^m y_{i,k-1}, \ \ \forall\, m, k \neq 1 \tag{2.35}$$

$$\bar{u}_k^m = \sum_{i=1}^{N_p} u_{ss}^m y_{i,\mathrm{k}}, \ \ \forall\, m, k \tag{2.36}$$

$$x_{k,e=1}^n = x_{in,k}^n \tag{2.37}$$

$$x_{k,N_e}^n = x_{in,k+1}^n, \ \ \forall k \neq N_s \tag{2.38}$$

$$x_{k,N_e}^n = x_{in,1}^n, \ \ \forall k = N_s \tag{2.39}$$

2.2.7 Lower and Upper Bounds of the State and Manipulated Variables

In constraints 2.40 and 2.41, we set lower bounds and upper bounds to the x_{ke}^n and u_{ke}^m respectively..

$$x_{min}^{n} \leq x_{ke}^{n} \leq x_{max}^{n}, \quad \forall n, k, e \qquad 2.40$$

$$u_{min}^{m} \leq u_{ke}^{m} \leq u_{max}^{m}, \quad \forall n, k, e \qquad 2.41$$

Chapter 3 Influence Brought by the Incorporation of Uncertainties

Works have been done to study the influence brought by the uncertainties and minimize it. However, majority of those works deal with the uncertainties in scheduling model or process control model. Few works focused on the uncertainty treatments of integration model of scheduling and control. The purpose of this work is to study the influence brought by the uncertainties of the integration model and to apply appropriate uncertainties treatment to minimize the influence. In this chapter, we incorporate the uncertain parameters which used to be treated as constant and analyze the corresponding influence brought by those uncertainties.

3.1 Influence Brought by the Incorporation of Uncertain Kinetic Parameter K

It is common that the values of some parameters in the dynamic models are obtained from theoretical calculation, experimental measurement, or a combination of those two methods. However, the implementation of those methods can hardly avoid bringing in errors, which can be considered as uncertainties of the dynamic model. As one of the most important parameters of the dynamic model, the kinetic parameter K is obtained by both experimental measurement and theoretical calculation. In this part, in order to know the influence that uncertain K brings to the deterministic integration model, we incorporate it into the model as the only uncertainty.

Programming the integration model of scheduling and control in GAMS and solving it with SBB solver, we observe that the deterministic integration model has a feasible region of kinetic parameter K, which is shown in expression 3.1. We observe that when the value of K falls below its lower bound, the corresponding reaction rate is too low to achieve high conversion, even with the lowest value of the flow rate. This phenomenon causes the system cannot reach the high conversion requirement of specific product, such as product A. Comparatively, when the value of K exceeds its upper bound, the relative reaction rate is too high to obtain low conversion, even though the flow rate reaches its highest value, the system fails to meet the low conversion requirement of some products, such as E. In those two scenarios, the integration model will fail to obtain the optimal solution because the demand constraints are violated.

$$K \in \left[1.935,\ 2.438\right] L^2/mol^2h \tag{3.1}$$

3.1.1 Influence on Optimal Production Sequence

By inputting different values of K within that region, we obtain the corresponding optimal solutions. From many values of kinetic parameter we input into the integration model, we choose the special values of K and corresponding optimal production order, and listed them in that Table 3.1 as follows. We divide the whole region into five periods, based on the production sequence we get from the integration model, within each slot, the production order will be stable. During the trial, there are two production sequences, D-C-B-A-E and D-E-C-B-A. We also discover that those two production orders are favored in turns. From Figure 3.1 to 3.5, we obtain sample values of K in each period and plot the figure of state and manipulated variables, which can demonstrate the phenomena more intuitively.

Table 3.1 Influence on Objective Function and Production Sequence

Periods	K	1st Slot	2nd Slot	3rd Slot	4th Slot	5th Slot
1	1.935	D	C	B	A	E
	1.94					
2	1.95	D	E	C	B	A
	1.97					
3	1.98	D	C	B	A	E
	2					
4	2.05	D	E	C	B	A
	2.051					
5	2.1	D	C	B	A	E
	2.438					

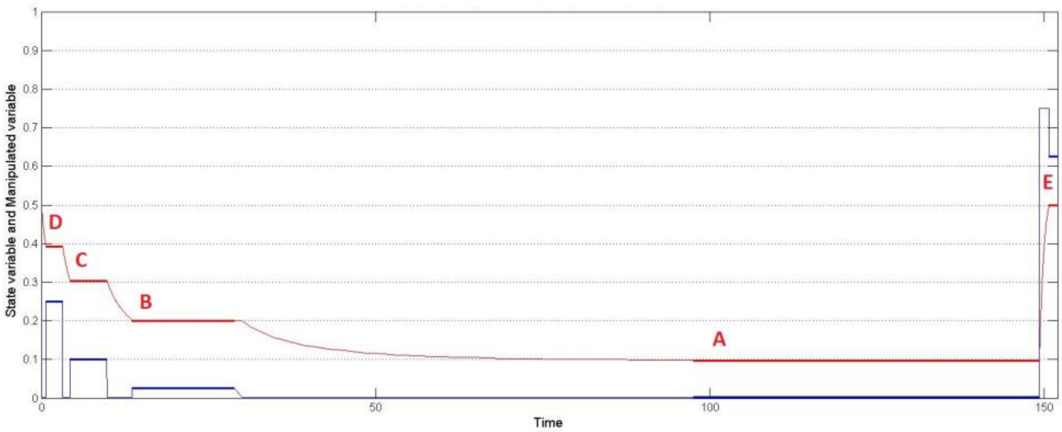

Figure 3.1 State Variable (Red) and Manipulated Variable (Blue) vs. Time,

while $K = 1.935\ L^2/mol^2h$, Period 1

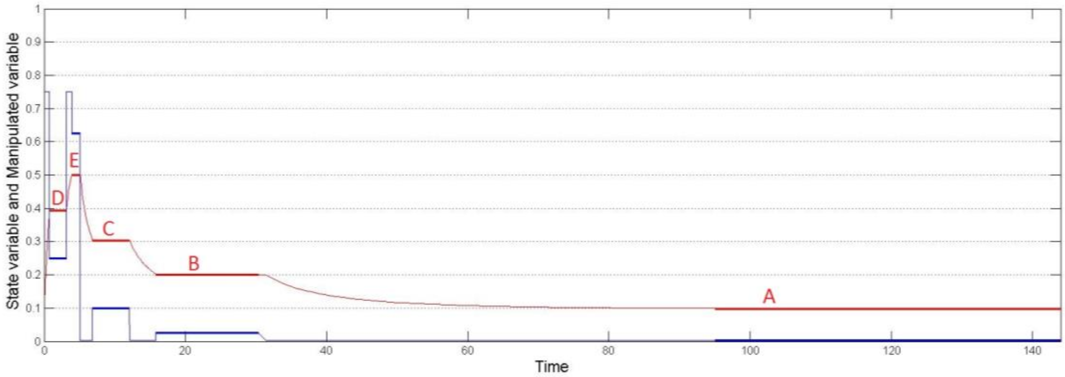

Figure 3.2 State Variable (Red) and Manipulated Variable (Blue) vs. Time,

while $K = 1.950\ L^2/mol^2h$, Period 2

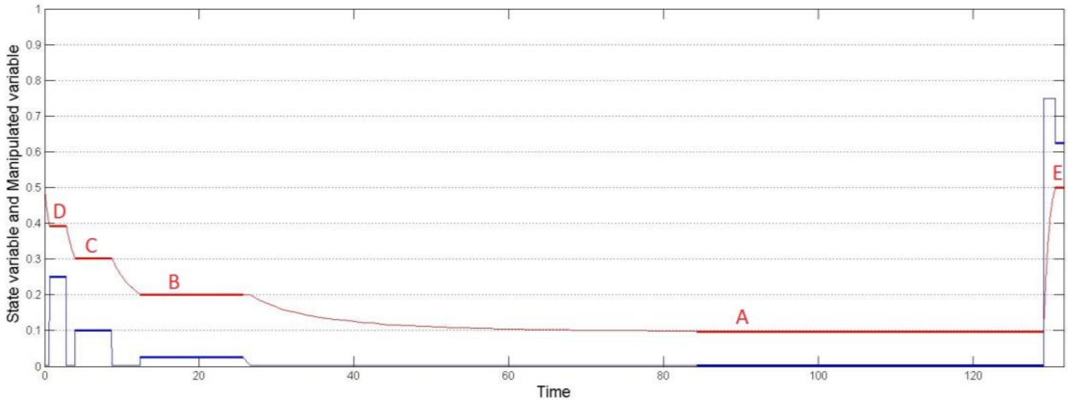

Figure 3.3 State Variable (Red) and Manipulated Variable (Blue) vs. Time,

while $K = 1.980\ L^2/mol^2h$, Period 3

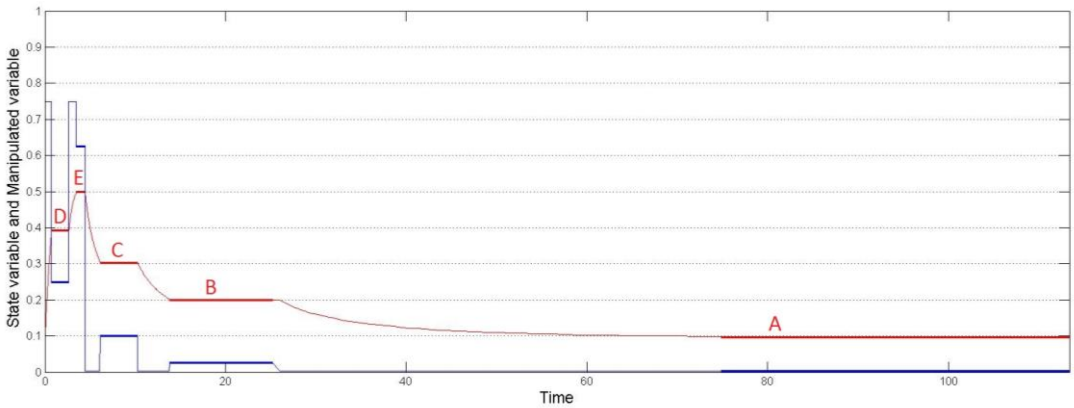

Figure 3.4 State Variable (Red) and Manipulated Variable (Blue) vs. Time,

while $K = 2.050\ L^2/mol^2h$, Period 4.

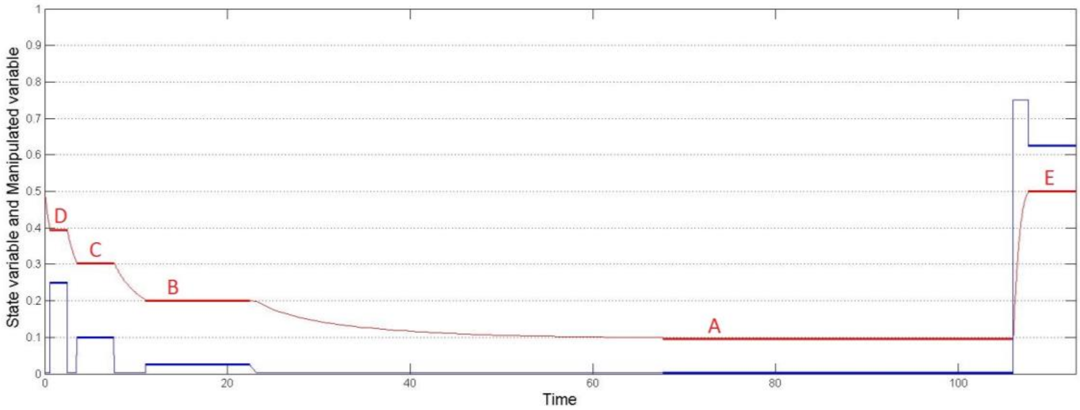

Figure 3.5 State Variable (Red) and Manipulated Variable (Blue) vs. Time,

while $K = 2.100\ L^2/mol^2h$, Period 5

3.1.2 Influence on Optimal Solutions

Solving deterministic integration models with different values of kinetic parameter K, we obtain the optimal solutions. The core index of the optimal solution consists of three parts: an optimal production sequence, optimal profit rate and corresponding time index.

Acting as a significant index of profit rate change and process time change, the variation of the production rate plays an important role in the sensitivity analysis. As plotted in Figure 3.6, we observe that with the increment value of kinetic parameter K, the production rate of product A, B, C and D decrease gradually. It is obvious that the production amount of E decreases gradually until $K = 2.051\ L^2/mol^2h$, and then the production rate of E starts to increase dramatically. By K reaching the highest value, the corresponding value of production rate of E increase nearly 20 times as $K = 2.051\ L^2/mol^2h$. The booming of the E production is a combined result of K

increment and highest value of desired manipulated variable. This would be analyzed more detailed later in this chapter.

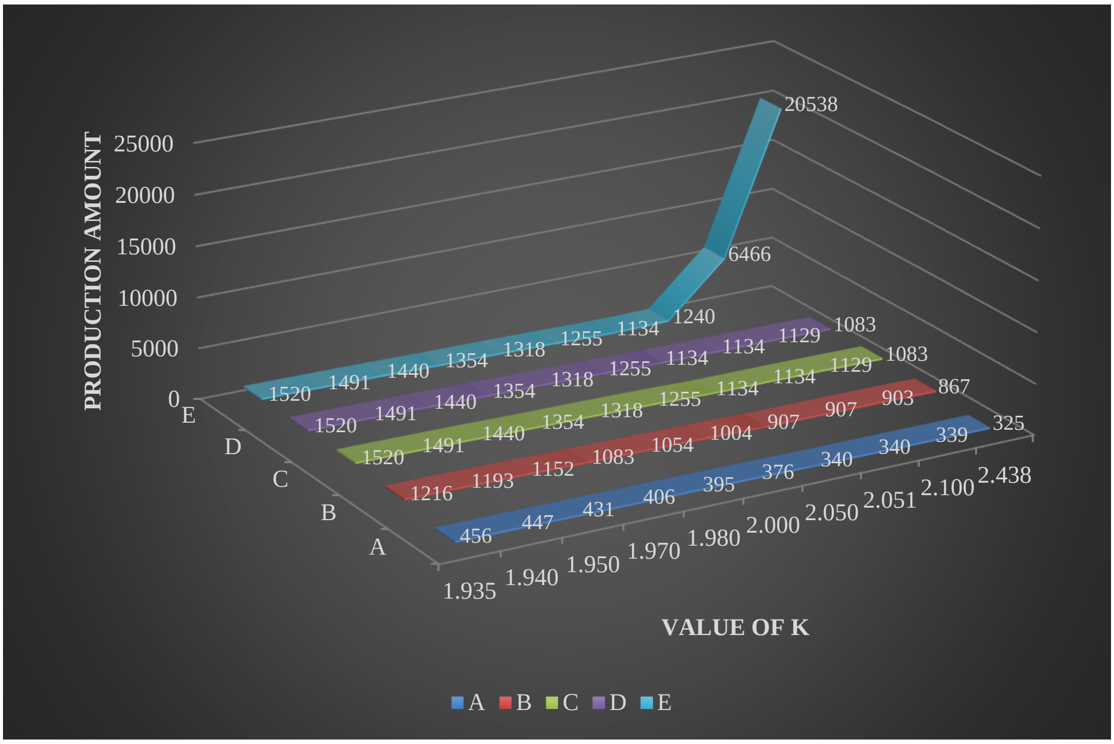

Figure 3.6 Influence on Production Rate under Uncertain K

The objective function of the integration model is the value of total profit rate, in other words, the purpose of the integration model is to maximize the total profit rate. We have the figure of profit rate of each product and the total profit rate in Figure 3.7. While the value of K is increasing, the trend of the profit rate change is increasing. We observe that profit rate of A, B and C increase gradually with the increment of K. Comparatively, the change trend of product D and E is affected by both increment of K and the change of production sequence. The dramatic increment of profit rate of E starts when $K = 2.051\ L^2/mol^2h$. Both increment value of K and its highest value of desired manipulated variable caused the profit rate of E increase much faster than the other products. The dramatic increment of profit rate increment of E resulted in its booming of production we mentioned before.

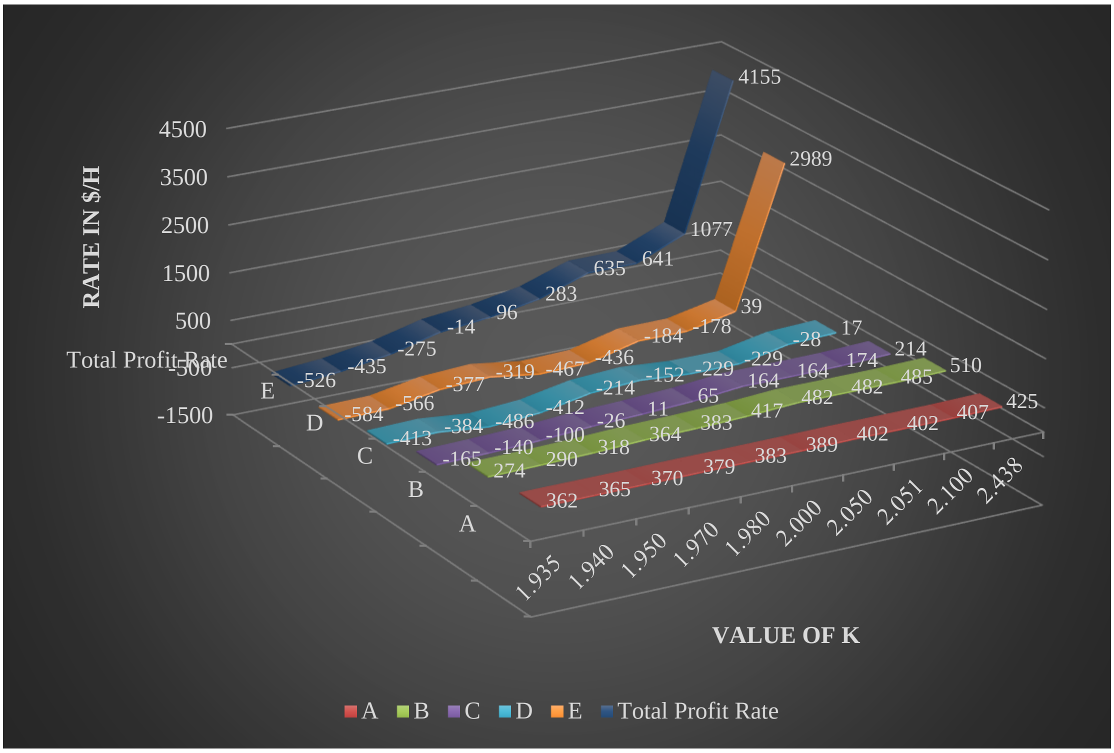

Figure 3.7 Influence on Profit Rate under Uncertain K

Another crucial index of this chemical process is the time variables. In this part, we focus on the slot time, the summation of transition time and production time, of each product and the corresponding cycle time, which are plotted in Figure 3.8. Combining the information of desired manipulated variables in Table 2.1 and the figures in Figure 3.8, it is easy to observe that the higher concentration of the reaction product and lower desired manipulated variable value the product need, the longer slot time the process need. For example, with concentration of reaction product $0.9033\, mol/L$ and a desired feeding rate of $10\, L/h$, the production of A consists of more than half of the cycle time. With the increment of K, the slot times of product A and B, and cycle time decrease gradually. The slot time change of C and D are decreasing while the value of K is increasing, but it is obvious that the change of slot time of Product C and D are also affected by the production sequence. As to product E, the slot time of E decrease until K exceeds $2.051\,L^2/mol^2h$, then it turns into dramatic increment. The abnormal behavior of slot time of E is mostly resulted by the highest value of desired manipulated variable.

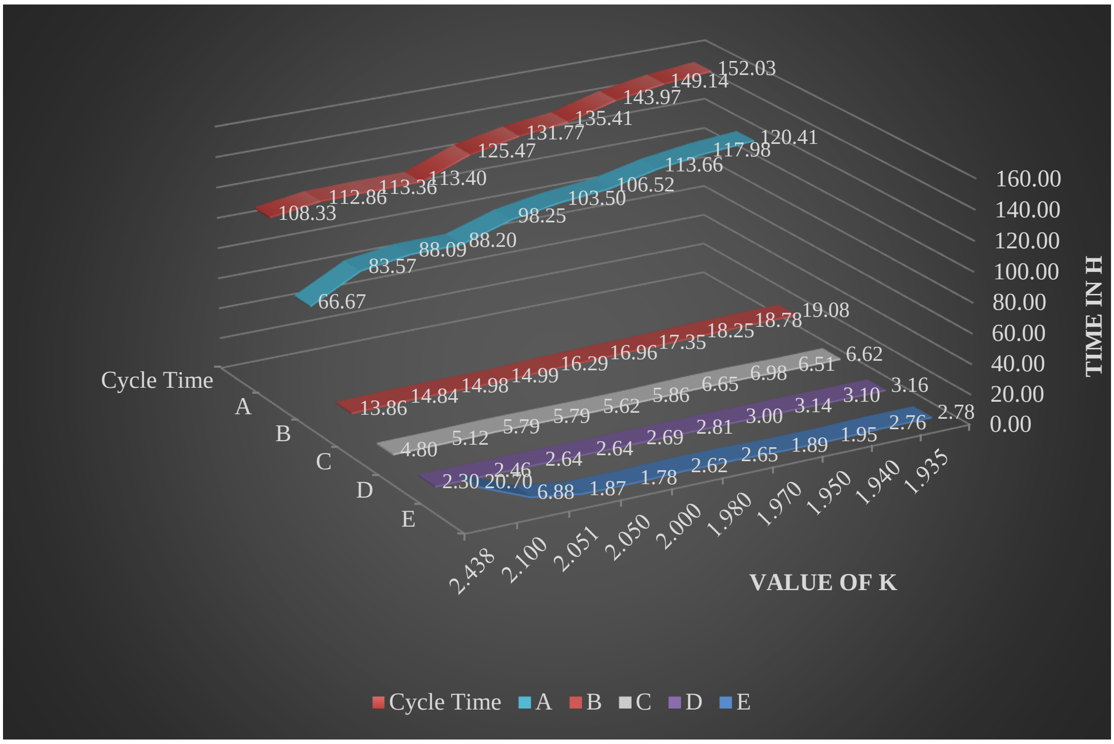

Figure 3.8 Influence on Slot Time and Cycle Time under Uncertain K

3.2 Influence brought by the Incorporation of Uncertain Initial Concentration of Reactant C_0

In the deterministic integration model, the initial concentration of the reactant C_0 is assumed to be constant. However, in actual industrial situations, C_0 of the production cycle can hardly be assured. For example, even though the process is capable of injecting reactant mixture into the CSTR with relatively stable concentration, tiny difference between the actual value and the desired value can hardly be avoided. Those tiny uncertainty will affect the optimal solution of the whole process. In order to make the integration model closer to the reality, we should simulate this phenomenon by incorporating the possible uncertainty brought by C_0.

In this part, we assume that C_0 is the only uncertainty incorporated into the consideration. Programing in GAMS and solving the deterministic integration model by SBB solver, we observe that breadth of the region of C_0 value is quite large. Even though the deterministic model is capable of obtaining optimal solutions while the value of C_0 exceeds that region, the difference between the desired value of C_0 and the actual value of C_0 should not be that severe during the industrial situation. Therefore, we assume that the region of the possible value of C_0 as follows.

$$C_0 \in [0.920,\ 1.030]\ mol/L \qquad 3.2$$

3.2.1 Influence on Optimal Production Sequence

Solving the deterministic integration model with different values of C_0, we obtain the optimal solutions. We pick the special values based on the production order of the corresponding optimal solution. As shown in the Table 3.2, we classify the whole range into 5 periods, based on the production sequence of the optimal solutions. While C_0 is the only uncertainty of the integration model, we also observe the rapid change of the optimal production sequence. The optimal production sequence could be classified into two categories: D-C-B-A-E and D-E-C-B-A.

Table 3.2 Influence on Objective Function and Production Sequence

Periods	C0	1st Slot	2nd Slot	3rd Slot	4th Slot	5th Slot
1	0.92	D	C	B	A	E
	0.96					
2	0.97	D	E	C	B	A
	0.99					
3	0.999	D	C	B	A	E
	1					
4	1.01	D	E	C	B	A
	1.025					
5	1.026	D	C	B	A	E
	1.03					

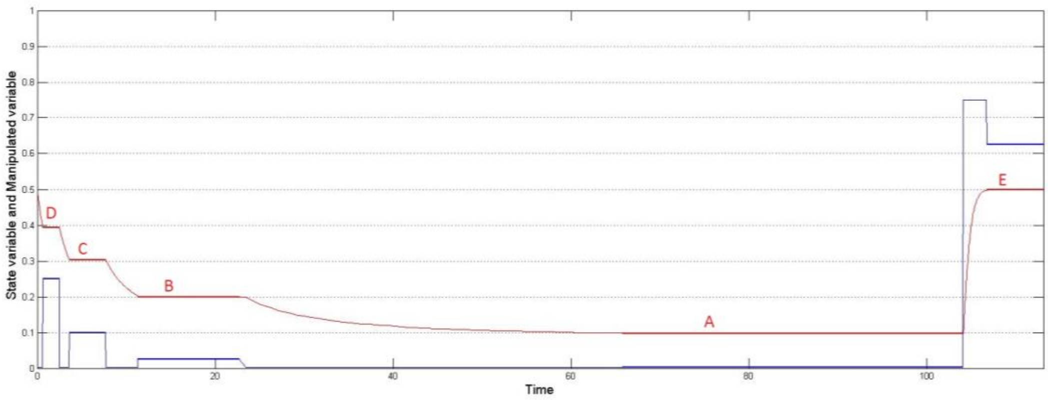

Figure 3.9 State Variable (Red) and Manipulated Variable (Blue) vs. Time, while $C_0 = 0.92\ mol/L$, Period 1

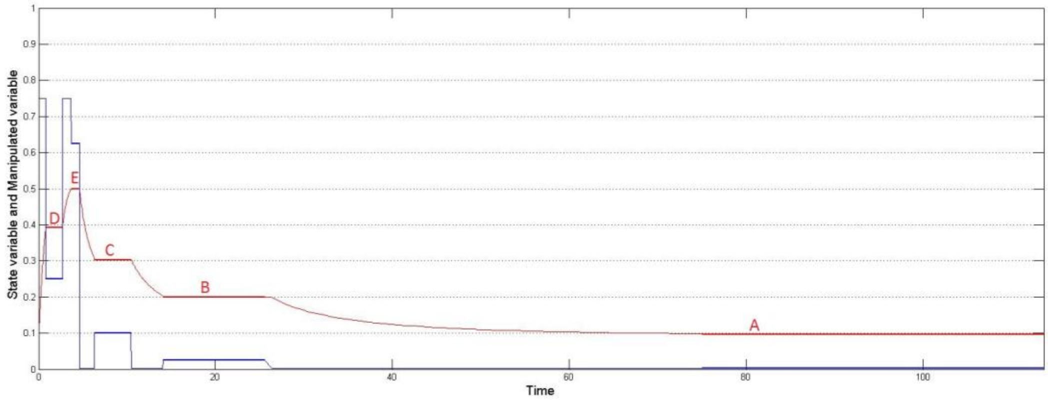

Figure 3.10 State Variable (Red) and Manipulated Variable (Blue) vs. Time,

while $C_0 = 0.97\ mol/L$, Period 2

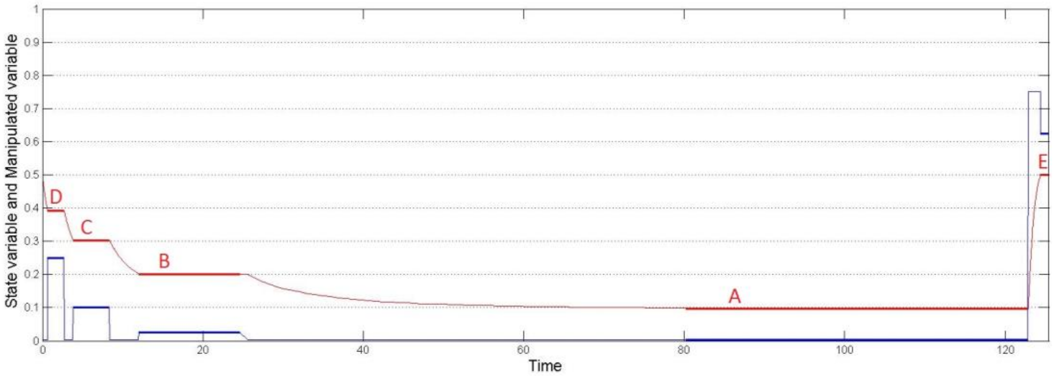

Figure 3.11 State Variable (Red) and Manipulated Variable (Blue) vs. Time,

while $C_0 = 1\ .00 mol/L$, Period 3

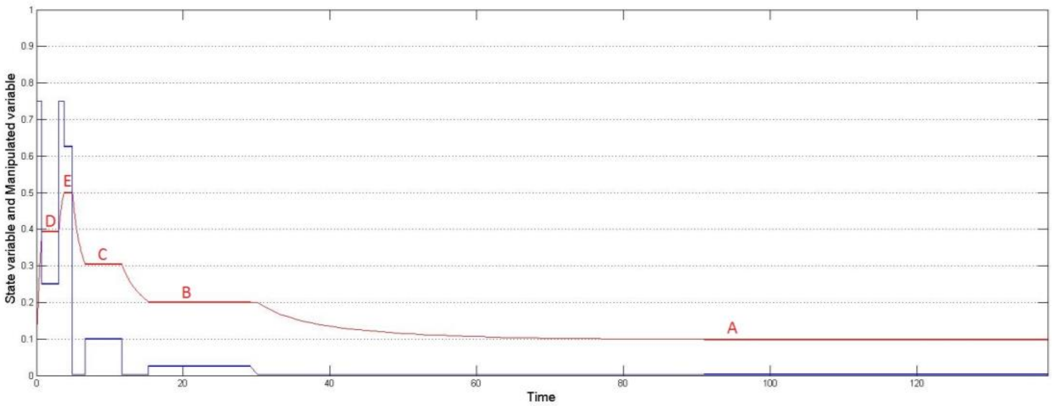

Figure 3.12 State Variable (Red) and Manipulated Variable (Blue) vs. Time,

while $C_0 = 1.02\ mol/L$, Period 4

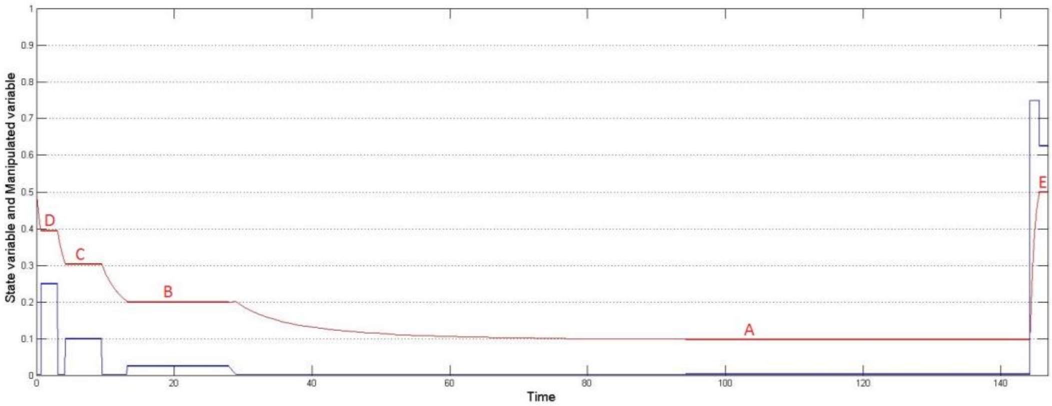

Figure 3.13 State Variable (Red) and Manipulated Variable (Blue) vs. Time, while $C_0 = 1.03\ mol/L$, Period 5

3.2.2 Influence on Optimal Solutions

Solving deterministic integration models with different values of initial concentration of reactant C_0, we obtain the optimal solutions. As mentioned in the last chapter, we still spread the analysis of influence on optimal solutions from three aspects: the optimal production sequence, optimal profit rate and corresponding time index.

In the Figure 3.14, we plot the value of production amounts of each product with respect to different values of C_0. While the value of C_0 is decreasing, the production amount of product A, B, C and D decrease gradually. When C_0 decreases, in order to obtain the highest profit rate, the integration model shrinks the production amount to minimize the inventory cost. The production amount of product E decrease gradually until the value of C_0 reaches $0.969\ mol/L$. While C_0 exceeds $0.969\ mol/L$ the production amount of E start to increase dramatically. The reason why the production of E shows abnormal is combined, which we will analyze it later in this chapter.

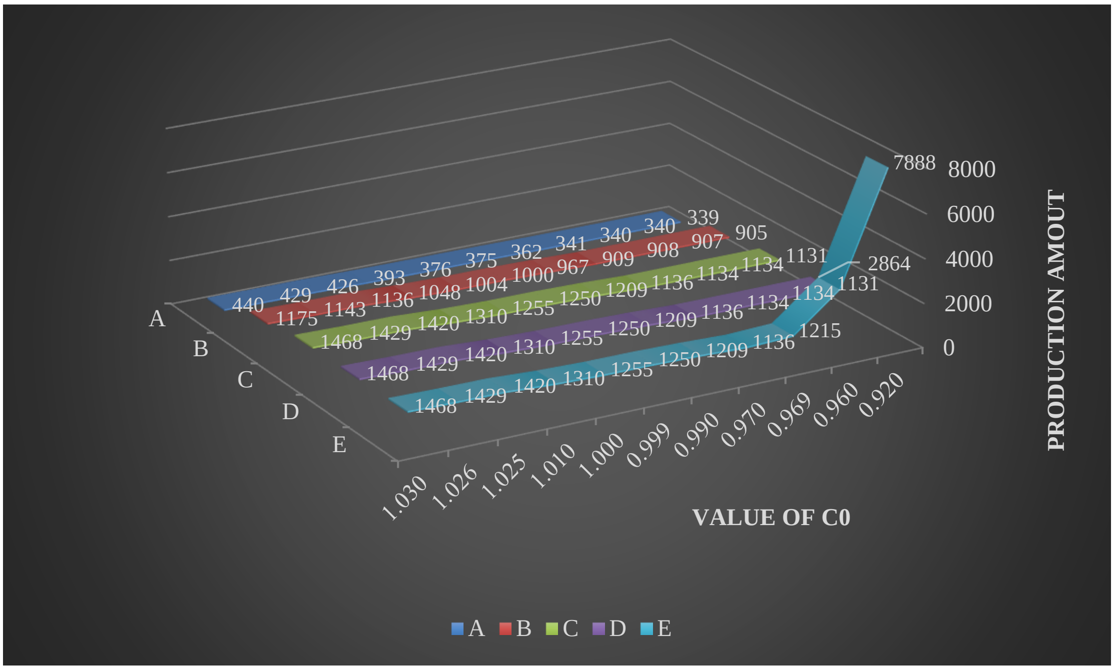

Figure 3.14 Influence on Production Amount under Uncertain C_0

As shown in Figure 3.15, we plot the profit rate of each product and the corresponding total profit rate of the system with respect to the different values of C_0. The profit rate of A, B and C increase gradually while the value of C_0 in decreasing. It is obvious that the production sequence affects the change of profit rate of C, D and E, especially for product D and E. Even though the profile of total profit rate shows a tendency of increasing with the decrement of C_0, we also observe the influence brought by the change of production sequence. The dramatic increment of E production while the value of C_0 is lower than $0.969\,mol/L$ dues to the production sequence and its higher increment in profit rate compared to the other products.

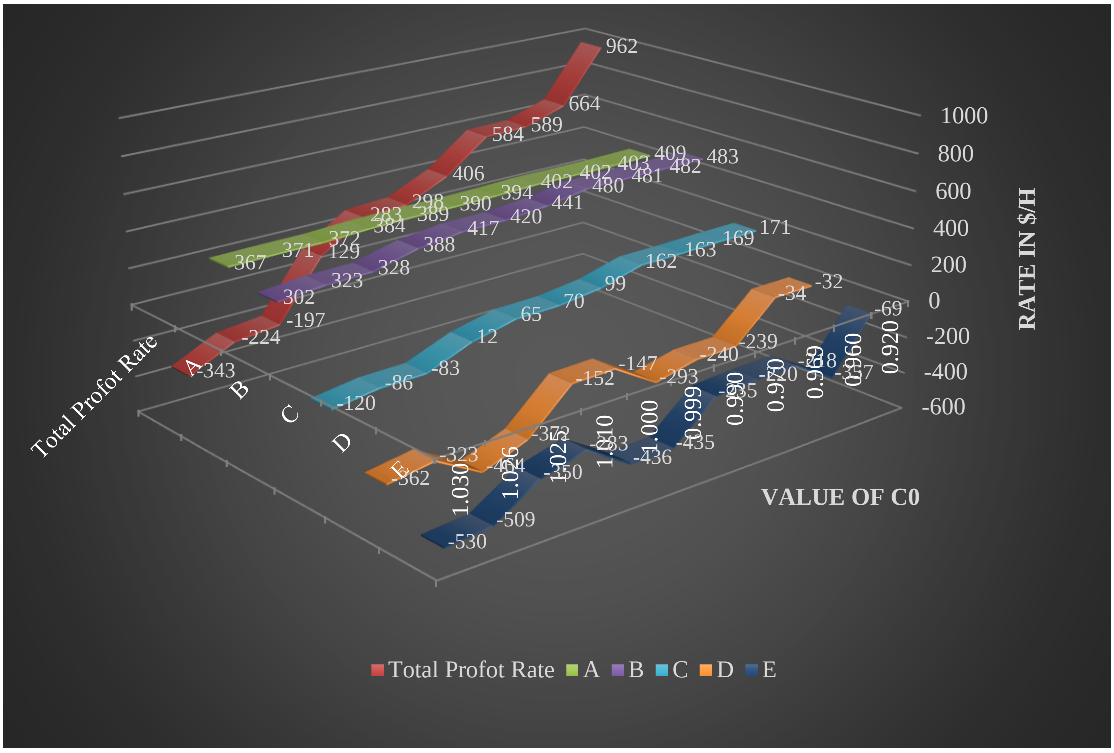

Figure 3.15 Influence on Profit Rate under Uncertain C_0

The profile of slot time of each product and the corresponding cycle time are plotted in Figure 3.16. The slot time of product A , B and the cycle time decrease while the value of C_0 is decreasing. The decrement of production amount leads to the decrement of slot time and cycle time. We also observe that the slot time of product C, D and E are affected by the change of the production sequence. The tendency of slot time change of C and D is still decreasing. As to slot time of product E, it decrease with the effect of change of production sequence, and turn into increasing when C_0 is lower than 0.969 mol/L, which is caused by the dramatic increment of production amount of E.

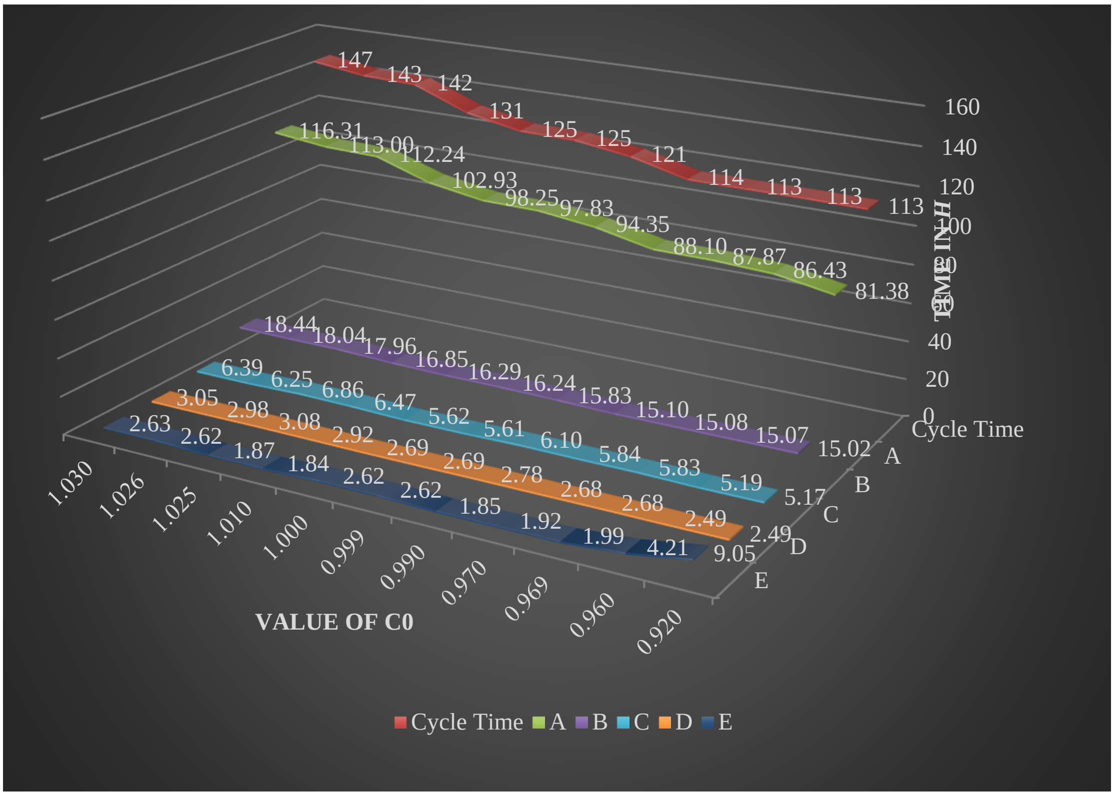

Figure 3.16 Influence on Slot Time and Cycle Time under Uncertain C_0

Chapter 4 Uncertainty Treatment

In this part, we will take both uncertainties into consideration and apply a scenario based method of uncertainty treatment to minimize the influence brought by the uncertainties. In order to revise the integration model closer to reality, we need to face three main problems summarized from the former chapters: (1) The integration model should stabilize the production amount and cover the realistic inventory equipment constraints under the influence of uncertainties; (2) The production assignment of the process should be determined regardless of the influence brought by the incorporation of uncertainties; (3) The optimal solution of the integration model should be steady and capable of measuring the benefit of the process under the influence of possible uncertainties.

4.1 Inventory Constraints

The dramatic increment of production amount of E when K obtained a high value or C_0 obtained a small value resulted in a dramatic increment of the profit rate. Apparently, it seems to be promising, however, it is hardly to achieve realistically because the model oversimplified the capability of inventory capacity in reality. In order to cover the realistic inventory capability in the integration model, we assume that there is an upper bound of the inventory capacity of each product, which is $2000\ kg$.

$$\left(G_i - {W_i}/{T_c}\right)\Theta_i \leq 2000 \qquad 4.1$$

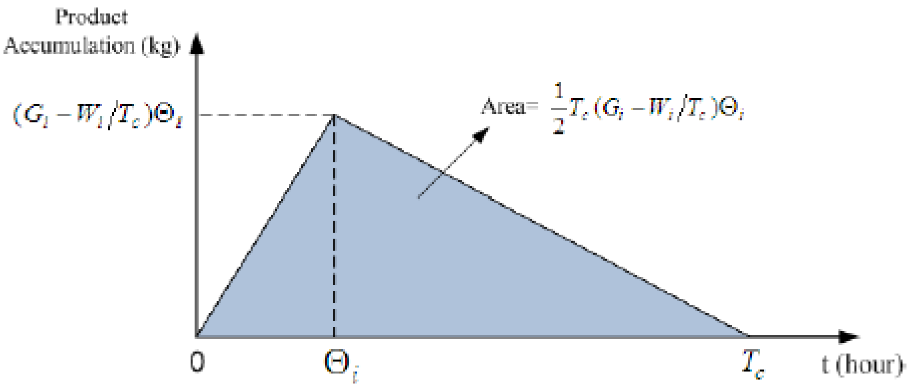

Figure 4.1 Inventory Constraints

4.2 Incorporation of Both Uncertain K and C_0

In reality, the uncertainties coexist simultaneously. Therefore, instead of incorporating one uncertainty into the integration model, we should take both uncertain kinetic parameter K and initial concentration of reactant C_0 into the consideration at the same time. We determine the C_0—K region of the integration model, in which we implement the uncertainty treatments. As the work we conducted in the chapter 3, we program the integration model with inventory constraints in GAMS and solve the model with SBB solver. We set the kinetic parameter and seek for the region of initial concentration of reactant. After repeating several times, we obtain the C_0—K feasible region of the integration model which is shown in the Figure 4.2.

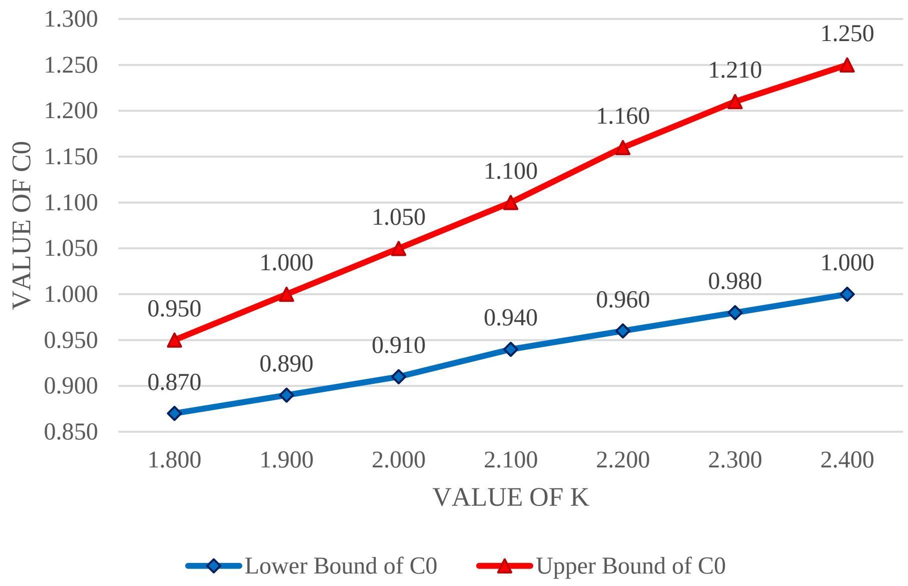

Figure 4.2 $C_0 - K$ Feasible Region of the Integration Model

4.3 Scenario Based Method

In chapter 3, we incorporated two uncertainties distinctively into the integration model to study the influence brought by each uncertainty. From the data we present, it is obvious that the integration model is quite sensitive to the uncertain kinetic parameter and the initial concentration of reactant. Under the influence of those uncertainties, the outcomes of integration model can hardly be regarded as stable, which prohibits the practical application of the integration of scheduling and control in reality. In this part, we apply a scenario based method to minimize the impact brought by the incorporation of the uncertainties.

4.3.1 Reformulation of the Integration Model

By introducing a new index s to the integration model, which indicates the scenarios that the integration model may obtain under the uncertainties, we reformulate the integration model to obtain a stable optimal production sequence and optimal solution.

4.3.1.1 Objective Function

Taking the possible scenarios that kinetic parameter or initial concentration of reactant may obtain into the consideration, we revise the objective function which is shown in 4.2. Φ_{ω}, the new objective function indicates the weighted sum of total profit rate of possible scenarios. The weight associated with each scenario s is represented as $\omega_s \in [0, 1]$. In order to determine the values of ω_s, we should know the distribution of the uncertainties we focusing on and the number of the possible scenarios taken into the consideration. In this study, we assume that both uncertainties are evenly distributed with the corresponding feasible region. Therefore, the values of the ω_s are calculated as shown in the expression 4.3. $\Phi^{(s)}$, obtained in equation 4.4, represents the total profit rate while the reaction system is under scenario s. In different scenarios, the manipulated variable u_{ke}^{m}, production amount W_i, total processing time Θ_i, transition time θ_k^t, process time at slot k p_k and cycle time T_c will obtain various values, therefore, total revenue rate Φ_1, total inventory cost rate Φ_2 and total raw material cost rate Φ_3 also changes by different scenarios. Considering this phenomenon, we obtain those parameters by scenario separately. The corresponding expressions are listed from equation 4.5 to 4.7.

$$\Phi_{\omega} = \sum_{1}^{s} \omega_s \, \Phi^{(s)} \tag{4.2}$$

$$\omega_s = \frac{1}{s} \tag{4.3}$$

$$\Phi^{(s)} = \Phi_1{}^{(s)} - \left(\Phi_2{}^{(s)} + \Phi_3{}^{(s)}\right) \tag{4.4}$$

$$\Phi_1{}^{(s)} = \sum_{i=1}^{N_p} \frac{C_i^p W_i{}^{(s)}}{T_c{}^{(s)}} \tag{4.5}$$

$$\Phi_2{}^{(s)} = \sum_{i=1}^{N_p} \frac{1}{2} C_i^s \Theta_i{}^{(s)} \left(G_i - \frac{W_i{}^{(s)}}{T_c{}^{(s)}}\right) \tag{4.6}$$

$$\Phi_3{}^{(s)} = \frac{1}{T_c{}^{(s)}} [\sum_{k=1}^{N_s} \sum_{e=1}^{N_e} C^r h_k \theta_k^{t\,(s)} \left(u_{ke}^{1\;(s)} + u_{ke}^{2\;(s)} + u_{ke}^{3\;(s)} + \cdots + u_{ke}^{m\;(s)}\right) + \sum_{k=1}^{N_s} C^r p_k{}^{(s)} (\overline{u}_k^1 + \overline{u}_k^2 + \overline{u}_k^3 + \cdots + \overline{u}_k^m)] \tag{4.7}$$

4.3.1.2 Assignment Constraints

From the data we obtained from Chapter 3, the optimal production sequence shows sensitive to the value of the uncertain parameter K and C_0. While applying the integration model to the industrial production, we should not allow the production sequence changing under the influence of the uncertainties. Therefore, in the new integration model, we set the assignment constraints independent of the scenarios of uncertainties. While solving the new optimization problem, the integration model will obtain the optimal production sequence maximizing the weighted sum of the total profit rate among all the possible scenarios. The formulations are shown from Equation 4.8 to 4.13.

$$\sum_{k=1}^{N_s} y_{ik} = 1, \ \forall i \tag{4.8}$$

$$\sum_{i=1}^{N_p} y_{ik} = 1, \ \forall k \tag{4.9}$$

$$y'_{ik} = y_{i,k-1}, \ \forall i, k \neq 1 \tag{4.10}$$

$$y'_{i1} = y_{i,N_s}, \ \forall i \tag{4.11}$$

$$z_{ipk} \geq y'_{ik} + y_{pk} - 1, \ \forall i, p, k \tag{4.12}$$

$$z_{ipk} \leq y'_{ik}, \ \forall i, p, k \tag{4.13}$$

4.3.1.3 Demand and Inventory Constraints

Shown as 4.14, the production rate of the product i is calculated from the flow rate F^0 and conversion $1 - X_i$. In expression 4.15, W_i, the production amount of the product i obtains different values in different scenarios, since the value of process time of the product i ,Θ_i is different by scenario. As the cycle time T_c is also affected by the value of K or C_0, the constraint of demand is also different by scenario, which is listed in 4.16. Shown as expression 4.17, in order to prohibit the dramatic increment of any product, we incorporate the inventory equipment constraints into the integration model, the maximum amount of inventory is set to be $2000\ kg$.

$$G_i = F^0(1 - X_i), \ \forall i \tag{4.14}$$

$$W_i{}^{(s)} = G_i \Theta_i{}^{(s)}, \ \forall i \tag{4.15}$$

$$D_i T_c{}^{(s)} \leq W_i{}^{(s)}, \ \forall i \tag{4.16}$$

$$\left(G_i - {W_i}^{(s)} \middle/ {T_c}^{(s)}\right) {\Theta_i}^{(s)} \le 2000\,, \quad \forall i \qquad 4.17$$

4.3.1.4 Time Constraints

It is obvious that production related time indexes will be affected by the values of the kinetic parameter and the initial concentration of reactant in various scenarios. Therefore, we incorporate the scenarios into the process time θ_{ik}, production time of product i Θ_i, production time of slot k p_k, transition time in slot k θ_k^t, starting and ending time of slot k t_k^s and t_k^e. The related formulations are shown from 4.18 to 4.25.

$$\theta_{ik}{}^{(s)} \le \theta^{max} y_{ik}, \quad \forall i, k \qquad 4.18$$

$$\Theta_i{}^{(s)} = \sum_{k=1}^{N_s} \theta_{ik}{}^{(s)}, \ \forall i \qquad 4.19$$

$$p_k{}^{(s)} = \sum_{i=1}^{N_p} \theta_{ik}{}^{(s)}, \ \forall k \qquad 4.20$$

$$\theta_k^{t\,(s)} = \sum_{i=1}^{N_p} \sum_{p=1}^{N_p} t_{pi}^{t\ (s)}\, z_{ipk}, \ \forall k \qquad 4.21$$

$$t_k^{e\,(s)} = t_k^{s\,(s)} + p_k{}^{(s)} + \theta_k^{t\,(s)} \qquad 4.22$$

$$t_1^{s\,(s)} = 0 \qquad 4.23$$

$$t_k^{s\,(s)} = t_{k-1}^{e}{}^{(s)}, \ \forall k \ne 1 \qquad 4.24$$

$$t_k^{e\,(s)} \le T_c{}^{(s)}, \ \forall k \qquad 4.25$$

4.3.1.5 Dynamic Model and Discretization

It is in this part we incorporate the possible scenarios of kinetic parameter K and initial concentration of reactant C_0 into the dynamic part of the integration model. As shown in expression 4.26, as a result of incorporation of the uncertainty scenarios, state variable x_{ke}^{n} and manipulated variable u_{ke}^{m} obtain different values in different uncertainty scenarios. Therefore, by following the Method of Runge–Kutta Forth-Order, the intermediate discretization parameters ${K_1}_{ke}^{n}$, ${K_2}_{ke}^{n}$, ${K_3}_{ke}^{n}$ and ${K_4}_{ke}^{n}$ are also different by scenario, which are reformulated in 4.27 to 4.31. Presented in 4.32, the length of the element h_k is not affected by scenarios, because we still obtain same number of the elements during each transition period.

$$\dot{x}_{ke}^{n\,(s)} = \frac{u_{ke}^{m\,(s)}}{V}\left({C_0}^{(s)} - x_{ke}^{n\,(s)}\right) - K^{(s)} {x_{ke}^{n\,(s)}}^{3}\ , \forall n, k, e \qquad 4.26$$

$${K_1}_{ke}^{n\ (s)} = \dot{x}_{ke}^{n\,(s)} \qquad 4.27$$

$${K_2}_{ke}^{n\ (s)} = \frac{u_{ke}^{m\,(s)}}{V}\left({C_0}^{(s)} - \left(x_{ke}^{n\,(s)} + 0.5 h_k \theta_k^{t\,(s)} {K_1}_{ke}^{n\ (s)}\right)\right) - K^{(s)}\left(x_{ke}^{n\,(s)} + 0.5 h_k \theta_k^{t\,(s)} {K_1}_{ke}^{n\ (s)}\right)^{3}\ , \forall n, k, e \qquad 4.28$$

$${K_3}_{ke}^{n\ (s)} = \frac{u_{ke}^{m\,(s)}}{V}\left({C_0}^{(s)} - \left(x_{ke}^{n\,(s)} + 0.5 h_k \theta_k^{t\,(s)} {K_2}_{ke}^{n\ (s)}\right)\right) - K^{(s)}\left(x_{ke}^{n\,(s)} + 0.5 h_k \theta_k^{t\,(s)} {K_2}_{ke}^{n\ (s)}\right)^{3}\ , \forall n, k, e \qquad 4.29$$

$${K_4}_{ke}^{n\ (s)} = \frac{u_{ke}^{m\,(s)}}{V}\left({C_0}^{(s)} - \left(x_{ke}^{n\,(s)} + 0.5 h_k \theta_k^{t\,(s)} {K_3}_{ke}^{n\ (s)}\right)\right) - K^{(s)}\left(x_{ke}^{n\,(s)} + 0.5 h_k \theta_k^{t\,(s)} {K_3}_{ke}^{n\ (s)}\right)^{3}\ , \forall n, k, e \qquad 4.30$$

$${x_{k,e+1}^{n}}^{(s)} = x_{ke}^{n\,(s)} + \frac{1}{6} h_k \left({K_1}_{ke}^{n\ (s)} + 2{K_2}_{ke}^{n\ (s)} + 2{K_3}_{ke}^{n\ (s)} + {K_4}_{ke}^{n\ (s)}\right) \qquad 4.31$$

$$h_k = \frac{1}{N_e} \qquad 4.32$$

4.3.1.6 Initial Condition and System Continuity

Even though the values of state variables and manipulated variables vary in different scenarios, the desired state variables and manipulated variables stay still for they are calculated through solving an open-loop model. As listed from 4.33 to 4.38, the initial conditions and desired conditions are same to the original integration model. Shown in 4.39, the first value of the transition element of slot k is assigned. Shown in expression 4.40 and 4.41, the continuity between transition and production is ensured.

$$x_{in,1}^{n} = \sum_{i=1}^{N_p} x_{ss,i}^{n} y_{i,N_s}, \quad \forall n \qquad 4.33$$

$$x_{in,k}^{n} = \sum_{i=1}^{N_p} x_{ss,i}^{n} y_{i,k-1}, \quad \forall n\,, k \neq 1 \qquad 4.34$$

$$\bar{x}_{k}^{n} = \sum_{i=1}^{N_p} x_{ss,i}^{n} y_{i,\mathrm{k}}, \quad \forall n, k \qquad 4.35$$

$$u_{in,1}^{m} = \sum_{i=1}^{N_p} u_{ss,i}^{m} y_{i,N_s}, \quad \forall m \qquad 4.36$$

$$u_{in,k}^{m} = \sum_{i=1}^{N_p} u_{ss}^{m} y_{i,k-1}, \quad \forall\, m, k \neq 1 \qquad 4.37$$

$$\bar{u}_{k}^{m} = \sum_{i=1}^{N_p} u_{ss}^{m} y_{i,\mathrm{k}}, \quad \forall\, m, k \qquad 4.38$$

$$x_{k,e=1}^{n}{}^{(s)} = x_{in,k}^{n} \qquad 4.39$$

$$x_{k,N_e}^{n}{}^{(s)} = x_{in,k+1}^{n}, \quad \forall k \neq N_s \qquad 4.40$$

$$x_{k,N_e}^{n}{}^{(s)} = x_{in,1}^{n}{}^{(s)}, \quad \forall k = N_s \qquad 4.41$$

4.3.1.7 Lower and Upper Bounds of the State and Manipulated Variables

As the original integration model, the values of state and manipulated variables in all the scenarios should not exceed the corresponding feasible region.

$$x_{min}^{n} \leq x_{ke}^{n\ (s)} \leq x_{max}^{n}, \quad \forall n, k, e \qquad 4.42$$

$$u_{min}^{m} \leq u_{ke}^{m\ (s)} \leq u_{max}^{m}, \quad \forall n, k, e \qquad 4.43$$

4.3.2 Obtaining Possible Scenarios

In order to implement the scenarios based method to the integration model, we need to generate possible scenarios that can represent the C_0—K region. As marked before, both uncertain K and uncertain C_0 are distributed evenly within the feasible region. Therefore, we generate the possible scenarios based on the C_0—K region with an even distribution. As shown in Figure 4.3, the possible scenarios are chosen geometrically. Firstly, we plot the feasible region in Cartesian coordinates, whose vertical axis and horizontal axis are is value of C_0 in mol/L and value of K in L^2/mol^2h. The step length of K and C_0 are $0.100\, L^2/mol^2h$ and $0.100\, mol/L$. Secondly, based on the C_0—K region we plotted, generate the possible scenarios. We obtain the values of uncertain parameters at the center of the square as the representative values of the parameters of the corresponding scenario. If more than half area of the square is in the C_0—K region, we consider the corresponding scenario is a possible scenario of the system, otherwise, the scenario is classified infeasible. In this case, we choose 10 possible scenarios, which indicate the C_0 — K region with evenly distribution.

Different scenarios can represent specific industrial situation that he reaction system may obtain.

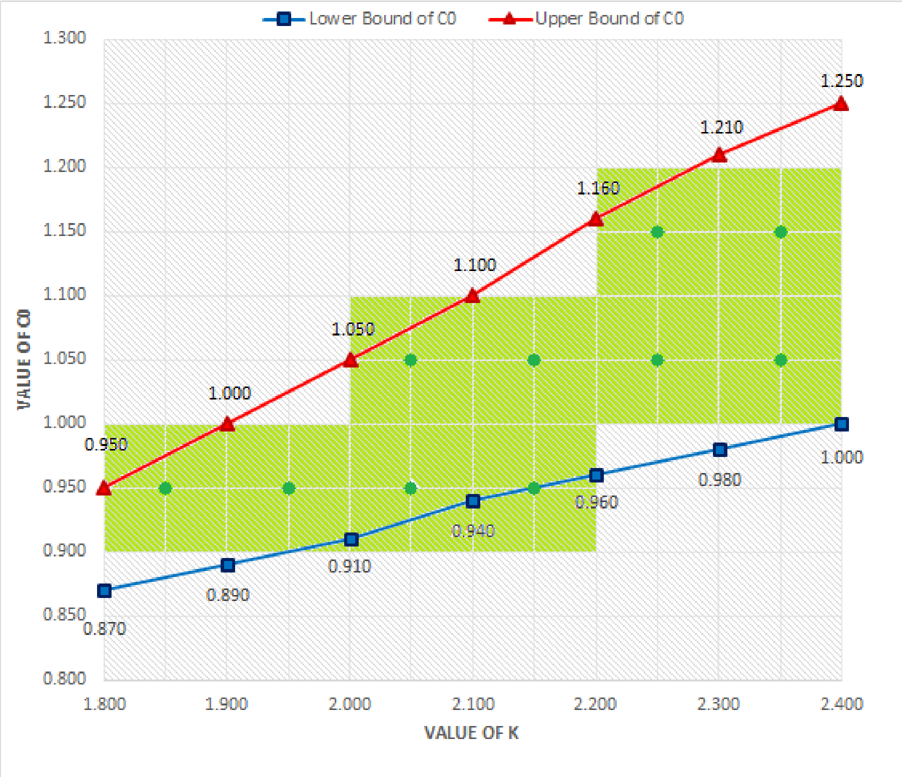

Figure 4.3 Obtaining Possible Scenarios from the C_0—K Region

Chapter 5 Results of Scenario Based Method within C_0—K Feasible Region of Uncertainty

In this work, we incorporate the uncertain kinetic parameter K and uncertain initial concentration of reactant C_0 into the integration model of scheduling and control of an isothermal multiproduct CSTR. By inserting different values of K and C_0, the deterministic integration model shows its instability. In order to make the integration model more realistic and applicable, we introduce inventory equipment constraints and implement a scenario based method of uncertainty treatment of the integration model. In this chapter, we evaluate the performance of the revised integration model of scheduling and control by comparing the optimal production sequence and optimal solutions to the deterministic integration model with different values of K and C_0.

Programing the revised integration model in GAMS and solving it by SBB solver, we obtain the optimal production sequence as D-B-C-E-A and its corresponding value of objective function is $61.57\ \$/h$. In order to compare the performance of the revised integration model, we run the corresponding deterministic integration model in each possible scenario the system might obtains. In order to compare the performance of the revised integration model, we list the total profits under each possible scenarios of the revised integration model and the corresponding optimal solution of the deterministic models in Table 5.1.

Table 5.1 Optimal Solutions of Revised Integration Model and the Corresponding Optimal Solutions of Deterministic Integration Models

Index of Scenario	**K**	**C0**	**Total Profit Rate of Revised Integration Model**	**Total Profit Rate of Scenarios of Revised Integration Model**	**Corresponding Deterministic Total Profit Rate**	**Optimal Production Order of Revised Integration Model**	**Corresponding Deterministic Production Order**
1	1.850	0.950	61.57	-1117.78	-455.43	D-B-C-E-A	D-C-B-A-E
2	1.950	0.950		-204.36	446.33		D-B-A-C-E
3	2.050	0.950		221.89	736.26		D-C-E-B-A
4	2.150	0.950		477.36	1267.49		D-C-A-B-E
5	2.050	1.050		-741.06	-122.61		D-E-B-C-A
6	2.150	1.050		169.34	804.64		D-E-B-C-A
7	2.250	1.050		679.19	1407.86		D-E-B-C-A
8	2.350	1.050		1134.23	1964.53		D-C-B-A-E
9	2.250	1.150		-453.15	127.57		D-E-B-C-A
10	2.350	1.150		450.07	1101.92		D-C-B-A-E

Firstly, we compare the optimal production sequence of the revised integration model and those of corresponding deterministic models. The optimal production sequence of the revised integration model is shared by all the possible scenarios, aiming at achieving the highest economic benefits under the consideration of 10 possible scenarios. Comparatively, the optimal production sequence of deterministic integration models is targeted at obtaining the highest objective function under a consideration of only one possible scenario. When the value of uncertainty changes, the operator of the process has to replace the value of the parameter and run the deterministic model again to obtain the production sequence, which is possibly different with the current one. The revised integration model can help the operators get rid of this situation. Within the possible scenarios, the operator only needs to input the possible values of uncertain parameters of possible scenarios once, and the revised integration model will come out a stable production sequence that can cover all those possible scenarios. As the value of objective function, we discuss is in the next paragraph.

Secondly, we focus on the value of the objective function. It is known that the revised integration model is solved only once and its objective function is a weighed summation of optimal total profit rates under each possible scenarios with one optimal production sequence. In other words, the optimal total profit rates of possible scenarios of the revised integration model are related. Comparatively, the optimal solutions of the deterministic integration models are not connected. By comparing the total profit rate of revised integration model in different scenarios with the corresponding optimal profit rates of deterministic integration model, we observe that the values of total profit rate of deterministic integration model are always higher than the corresponding total profit rate of revised integration model. The reason for this phenomenon is the revised integration model only obtains one optimal production sequence, which may not be the optimal production sequence if solved in the corresponding deterministic integration model. From the analysis we have, we conclude that the value of objective function of the revised integration model can provide a comprehensive prediction to evaluate the process under the uncertainties.

However, the scenario based method also has some disadvantages. It is obvious that the optimal solution of the revised integration model is more precise when taking as many as possible scenarios into the consideration, but it is unrealistic to accomplish for two reasons. Firstly, we need to have a comprehensive knowledge to describe the uncertainties and obtain possible scenarios accurately, which could be quite difficult in reality. Secondly, even though we are able to obtain large amount of possible scenarios accurately and representatively, to obtain a robust optimal solution, the corresponding exponential increment of calculation complexity and CPU time will become a severe problem.

Chapter 6 Future Work

We have implemented and evaluated the performance of the scenario based method to the integration model of an isothermal multiproduct CSTR, however, we also know its disadvantages. By analyzing the characteristics of the integration model, we might have other promising methods to incorporate the uncertainties into the integration model.

In order to obtain an integration model of scheduling and control, we need to restructure those two distinctive models into same type of optimization formulation. In this study, we focus on an isothermal multiproduct CSTR. The main reaction of the process is an irreversible reaction. The scheduling problem is an MINLP problem and the corresponding process control model is an MIDO problem. In order to integrate an MINLP problem and an MIDO problem, we discretize the control model through Runge–Kutta Forth-Order Method. The MIDO problem is transferred into an MINLP problem based on the nonlinear behavior of the state equation. As the objective functions of scheduling model and the process control model are all related to the total profit rate, it would be much easier to integrate the scheduling model and control model. The integration model of scheduling and control is constructed into an MINLP problem, whose objective function is the total profit rate of the process.

Introduced in the 1970's, Robust Optimization has developed for over 40 years.[12] As a special advantage of Robust Optimization, we can obtain a stable optimal solution under the influence of uncertainties without knowing much information about the uncertainty, such as the distribution of the uncertainty.[13] Therefore, it would be a great help for the operators when the information of uncertainties is unknown. Many works on Robust Optimization have been done recently, however, the Robust Optimization is implemented mostly to linear systems. Unfortunately, the dynamic equations of the vast majority of the actual reactions in reality are nonlinear. Some reactions are much more complicated than the nonlinear system we have in this study. Since Non-Liner Robust Optimization is extremely complex, some scientists have worked out some algorithms as compensates. As a very promising method, Discrete Robust Optimization is capable to obtain the optimal solution of a nonlinear optimization problem.

In order to solve the nonlinear system we have in this work, we can discretize the nonlinear system into a discrete system and implement Discrete Robust Optimization to the discrete system to obtain a robust optimal solution immunized to the uncertainties. However, Discrete Robust Optimization also have challenges. One of the most challenging processes is that it is difficult to find suitable discretization method to the nonlinear system keeping the dynamic behavior of the original system, because we need to consider the influence brought by the changing value of some parameters in the ordinary differential equation or partial differential equations.[14] Even though the mathematic process of this method would be much more complicated than scenario based method we applied in this work, Discrete Robust Optimization has a potential to output a robust optimal solution with very few information known, which is worthy to learn in the future.

Reference

1. Harjunkoski, Iiro, Christos T. Maravelias, Peter Bongers, Pedro M. Castro, Sebastian Engell, Ignacio E. Grossmann, John Hooker, Carlos Méndez, Guido Sand, and John Wassick. "Scope for industrial applications of production scheduling models and solution methods." *Computers & Chemical Engineering* 62 (2014): 161-193.

2. Li, Zukui, and Marianthi Ierapetritou. "Process scheduling under uncertainty: Review and challenges." *Computers & Chemical Engineering* 32, no. 4 (2008): 715-727.

3. Floudas, Christodoulos A., and Xiaoxia Lin. "Continuous-time versus discrete-time approaches for scheduling of chemical processes: a review." *Computers & Chemical Engineering* 28, no. 11 (2004): 2109-2129.

4. Shobrys, Donald E., and Douglas C. White. "Planning, scheduling and control systems: why cannot they work together." *Computers & chemical engineering*26, no. 2 (2002): 149-160.

5. Engell, Sebastian, and Iiro Harjunkoski. "Optimal operation: Scheduling, advanced control and their integration." *Computers & Chemical Engineering* 47 (2012): 121-133.

6. Harjunkoski, Iiro, Rasmus Nyström, and Alexander Horch. "Integration of scheduling and control—Theory or practice?." *Computers & Chemical Engineering* 33, no. 12 (2009): 1909-1918.

7. Baldea, Michael, and Iiro Harjunkoski. "Integrated production scheduling and process control: A systematic review." *Computers & Chemical Engineering* 71 (2014): 377-390.

8. Ben-Tal, A., L. El Ghaoui, and A. Nemirovski. "Robustness optimization." (2009).

9. Zhuge, Jinjun, and Marianthi G. Ierapetritou. "Integration of scheduling and control with closed loop implementation." *Industrial & Engineering Chemistry Research* 51, no. 25 (2012): 8550-8565.

10. Flores-Tlacuahuac, Antonio, and Ignacio E. Grossmann. "Simultaneous cyclic scheduling and control of a multiproduct CSTR." *Industrial & engineering chemistry research* 45, no. 20 (2006): 6698-6712.

11. Washington, Ian D., and Christopher LE Swartz. "Design under uncertainty using parallel multiperiod dynamic optimization." *AIChE Journal* 60, no. 9 (2014): 3151-3168.

12. Soyster, Allen L. "Technical note—convex programming with set-inclusive constraints and applications to inexact linear programming." *Operations research* 21, no. 5 (1973): 1154-1157.

13. Li, Zukui, and Marianthi G. Ierapetritou. "Robust optimization for process scheduling under uncertainty." *Industrial & Engineering Chemistry Research* 47, no. 12 (2008): 4148-4157.

14. Kastsian, Darya, and Martin Mönnigmann. "Robust optimization of fixed points of nonlinear discrete time systems with uncertain parameters." *SIAM Journal on Applied Dynamical Systems* 9, no. 2 (2010): 357-390.